Electronic Supplementary Material (ESI) for Dalton Transactions.

Supplementary Information

for

A Proton-Conductive Metal-Organic Framework Based on Imidazole and Sulphate Ligands

Fuqi Mi [a, b], Faxue Ma[b, c], Shuixiang Zou[a, b], Dongsun Zhan[a, b], Teng Zhang[b, d]

[a] *College of Chemistry and Materials Science, Fujian Normal University, Fuzhou 350007, China*

[b] *State Key Laboratory of Structural Chemistry, Fujian Institute of Research on the Structure of Matter, Chinese Academy of Sciences, Fuzhou 350002, China*

[c] *College of Chemistry and Chemical Engineering iCHEM, State Key Laboratory of Physical Chemistry of Solid Surface, Xiamen University, Xiamen 361005, China*

[d] *University of the Chinese Academy of Sciences, Beijing 100049, China*

1. Reagents and Apparatus

All chemicals and reagents were used as received from commercial sources without further purification. Powder x-ray powder diffraction (PXRD) was measured on the Miniflex600 Desktop X-ray Diffractometer using Cu-Ka radiation ($\lambda = 1.5418$ Å) with 1°/min and 0.02° scan width between 5° and 50°. Thermogravimetric (TG) measurement was operated on STA449F3 simultaneous thermal analyzer with the heating rate of 10 °C/min with nitrogen flow (50 mL/min). SEM images were taken with SU-8010 field emission scanning electron microscope with the secondary electron imaging resolution $\leq$ 1 nm (15 kV，XWD $\geq$ 4 mm) or $\leq$ 1.3 nm (1 kV). The elemental analysis (EA) was performed on a Vario EL-cube which stability controlled less than 0.3% and the repeatability less than 0.1%.

The CO_2 sorption isotherms were recorded on ASAP 2020 M. Water adsorption is performed on a Vstar automatic specific surface and porosity analyzer. Before sorption measurements, solvent exchange was carried out in methanol for 3 days, and the sample was placed in the sample large bulb glass sample cell and outgassed under vacuum at 100 °C for 10 h.

2. Synthesis

2.1 Preparation of 1,5-dihydrobenzo[1,2-d:4,5-d']diimidazole-2,6-dithiol (DHBDIT)

A mixture of 1,2,4,5-phenyltetramine hydrochloride (2.000 g, 7.04 mmol), potassium ethyl xanthate (4.974 g, 31.08 mmol), 95% anhydrous ethanol (48 mL) and water (32 mL) in a flask was heated to reflux for 3 hours. Activated carbon (2.000 g) was then added cautiously and the mixture was heated at the reflux temperature for another 20 minutes. After removing activated carbon by filtration, the filtrate was heated to again to 65 °C and 16 mL of warm tap water (60- 70 °C) was added, followed by 4 ml of acetic acid in 8 ml of water with stirring. The product was separated out as grey powder after cooling in a refrigerator overnight. The product is collected and vacuum-dried at 40 °C [1]. Yield: 0.83 g, 53%. ^{1}H NMR (400 MHz, DMSO-d_6) δ: 12.45 (s, 1H), 6.82 (s, 1H). ^{13}C NMR (100.7 MHz, DMSO-d_6) δ: 167.97, 129.14, 90.19.

2.2 Synthesis of $[Cu_2(DHBDI)_3(SO_4)_2]_n\cdot 3H_2O$

Copper(II) nitrate trihydrate (0.0621 mmol, 15 mg) and DHBDIT (0.027 mmol, 6 mg) was dissolved in a solvent mixture of deionized water (1 mL), methanol (0.5 mL), dimethyl sulfoxide (1.5 mL) and formic acid (5 μL). After heating at 100 °C for 72 h, the formed green crystals were collected and washed with N,N-Dimethylformamide (DMF) and water (yield: 2.3 mg, 65% based on the organic ligand). Anal. Calcd (%) for the sample after adsorption $[Cu_2(DHBDI)_3(SO_4)_2]_n\cdot 3H_2O$: C, 31.97; H, 3.35; N, 18.64. Found: C, 32.11 H, 2.88; N, 18.45.

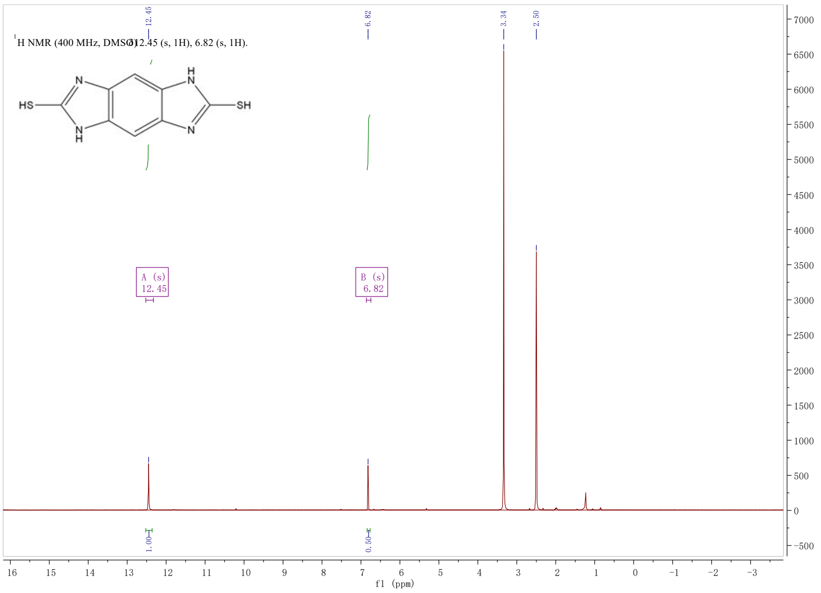

Figure S1. ^{1}H NMR spectrum of DHBDIT.

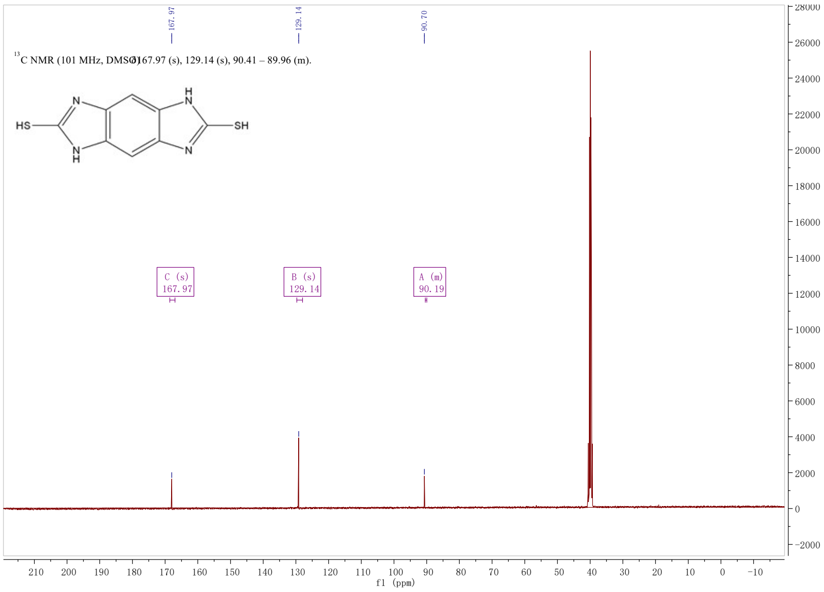

Figure S2. ^{13}C NMR spectrum of DHBDIT.

3. Single crystal X-ray crystallography

Single crystal X-ray diffraction of MOF **1** was carried on a Synergy Custom diffractometer, with Cu Kα radiation (λ = 1.54184 Å) at 100 K. The crystal structure was solved by intrinsic phasing and refined to convergence by full-matrix least-square fitting on F^2 using the SHELX-2019 software package. All non-hydrogen atoms were refined anisotropically. The hydrogen atoms on the aromatic rings were located at geometrically calculated positions and refined by "riding" modes. The diffused electron densities resulting from these solvent molecules were removed using the SQUEEZE routine of PLATON.

Single crystal X-ray diffraction of compound **2** was performed with a BRUKER D8 VENTURE equipped with Cu-Kα and Mo-Kα radiation. Mo Kα radiation was used. The frames were integrated with the Bruker SAINT© build in APEX III software package using a narrow-frame integration algorithm, which also corrects for the Lorentz and polarization effects. Absorption corrections were applied using SADABS. Structures were solved by intrinsic phasing and refined to convergence by least squares method on F^2 using the SHELX-2019 software suite. All non-hydrogen atoms are refined anisotropically. The hydrogen atoms on the aromatic rings were located at geometrically calculated positions and refined by "riding" modes.

Table S1. Crystal data and structure refinement for **1** and **2**.

Compound	**MOF 1**	**Compound 2**
Empirical formula	$C_{12}H_9CuN_6O_4S$	$CuC_{16}H_{16}N_8O_{12}S_2$
Formula weight	396.85	160.01
Temperature/K	100.15	249.95
Wavelength/ Å	1.54184	0.71073
Crystal system	orthorhombic	monoclinic
Space group	*Pbcn*	$P2_1/c$
a/Å	20.6518(4)	9.946(3)
b/Å	9.8071(2)	16.293(5)
c/Å	15.1637(3)	6.924(2)
α/°	90	90.00
β/°	90	91.321(15)
γ/°	90	90.00
Volume/Å^3	3071.17(11)	1121.8(6)
Z	8	8
ρ_{calc}/g·cm^{-3}	1.717	1.895
μ/mm^{-1}	3.589	1.245
F(000)	1600.0	650
Crystal size/mm^3	0.3 ×0.26 ×0.24	0.3 × 0.26 ×0.24
θ range data collection	4.282°-76.370°	2.400°-25.950°
Limiting indices	-17<=h<=25, -12<=k<=5, -18<=l<=19	-11<=h<=12, -18<=k<=19, -7<=l<=8
Reflection collected	11189	6382
Independent reflections	3109	2133
R(int)	0.026	0.136
Data/restraints/parameters	3109/0/217	2133/2/184
Goodness-of-fit on F^2	1.101	1.127
Final R indexes [I>=2σ(I)]	R_1 = 0.0757, wR_2 = 0.2535	R_1 = 0.0924, wR_2 = 0.2373
Final R indexes [all data]	R_1 = 0.0811, wR_2 = 0.2619	R_1 = 0.1538, wR_2 = 0.2770

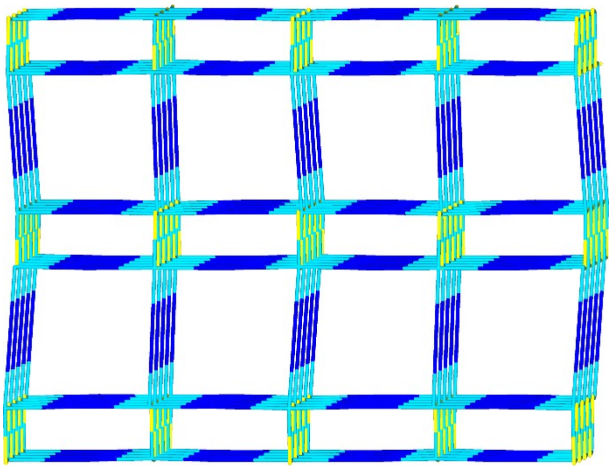

Figure S3. Schematic view of the topology framework of MOF **1**. For clarity, the linkers are displayed in three colors: the blue linkers represent the kinds of 2-connected ligands, the cyan linkers represent the kinds of 5-connected Cu centers, and the yellow linkers represent the kinds of 2-connected sulphate.

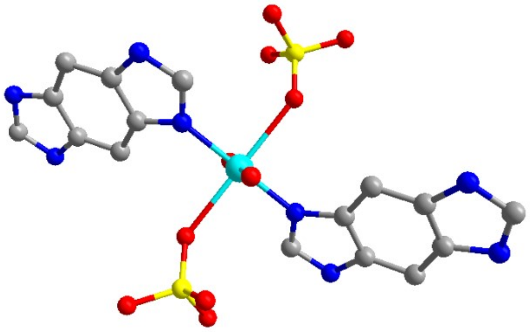

Figure S4. The crystal structure of Cu(HDHBDI)$_2$(SO$_4$)$_2$(H$_2$O)$_2$ (**2**).

4. Characterization of the MOF

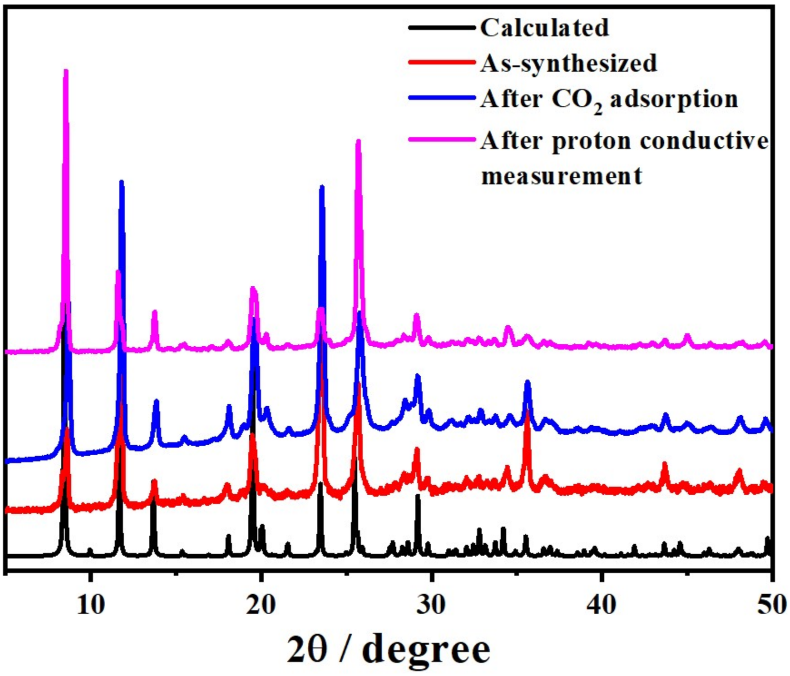

Figure S5. PXRD patterns before and after CO_2 adsorption/desorption test and proton conductive measurement for MOF **1**.

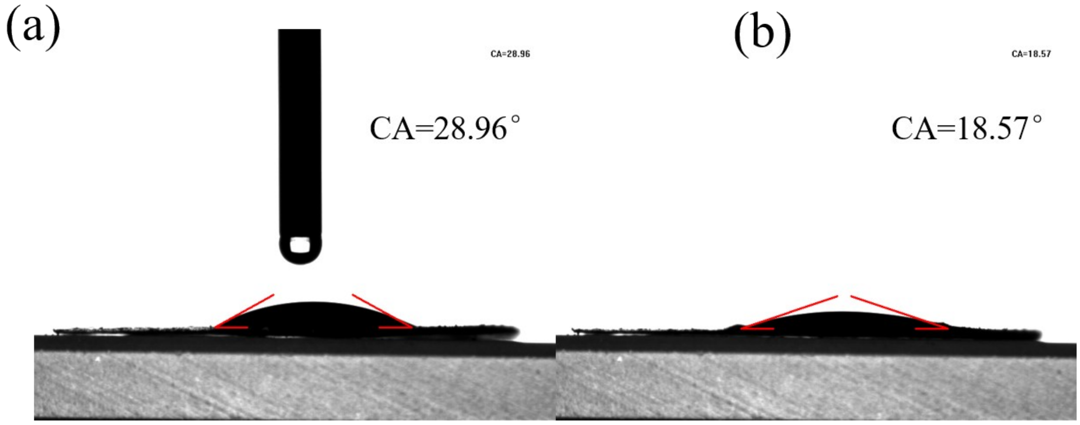

Figure S6. The water contact angle images of MOF **1** at first contact (a) and spread out (b).

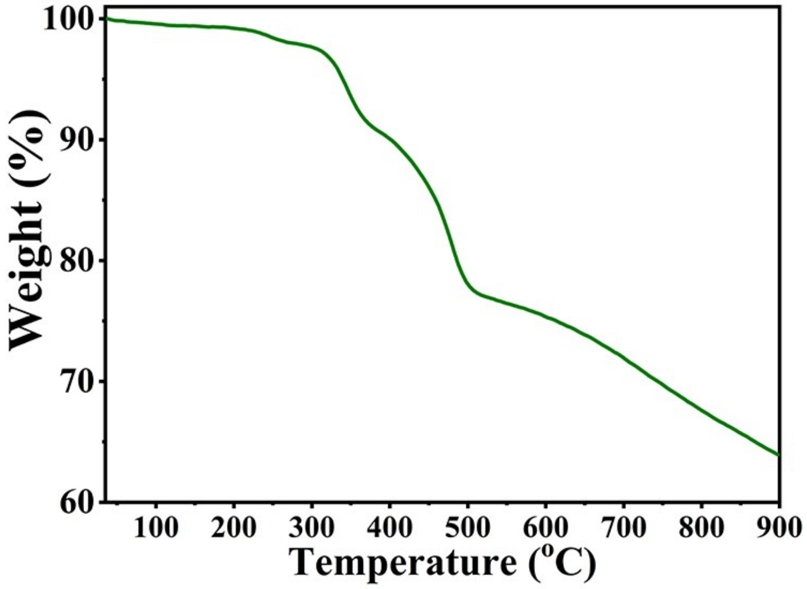

Figure S7. Thermogravimetric analysis curve of MOF **1**.

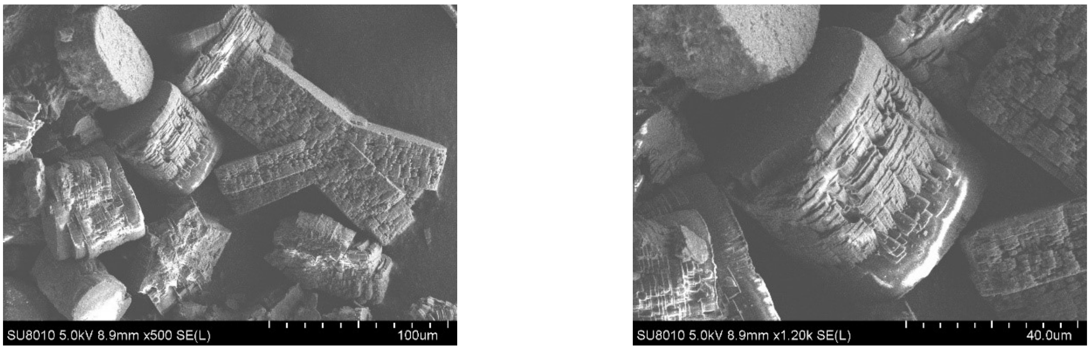

Figure S8. SEM images of MOF **1** before and after treated in boiling water.

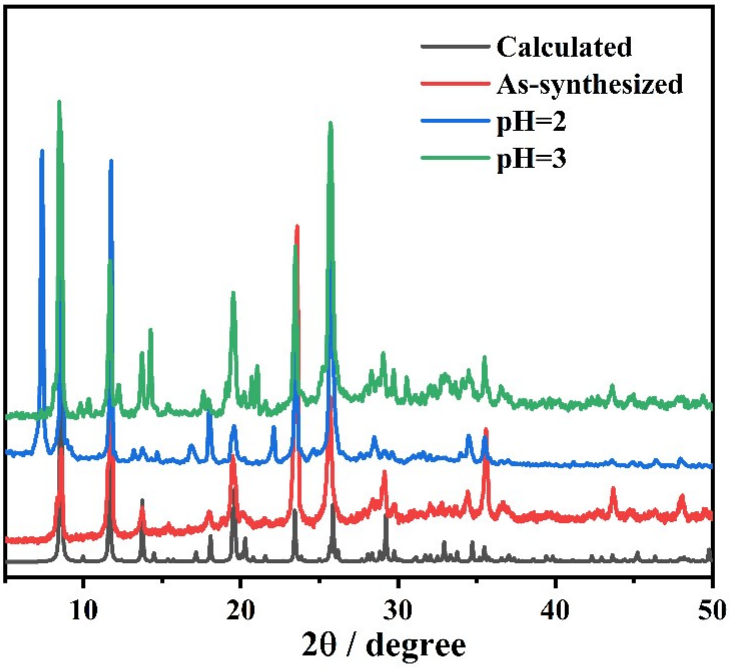

Figure S9. PXRD patterns of MOF **1** after soaked in pH=2 and pH=3 H_2SO_4 aqueous solution for 6 days.

5. Proton Conductivity Measurement

We use quasi-four-probe method with a Solartron SI 1260 Impedance Gain-Phase Analyzer test the impedance value of the material by applying 500 mV AC voltage whose frequency (ω) is swept from 1 to 1×10^7 Hz in 10 steps on a logarithmic scale under certain humidity and temperature environments. The model used to control humidity and temperature is XK-CTS80Z (ShenZhen selenium control testing equipment corp) humidity control oven. The powder material was pressed at the pressure of 2.3 Mpa for two minutes into a pellet with a thickness of 0.083 cm and a diameter of 0.25 cm. The diameter of the tablet pressing mold is the diameter of the sample pellet, and its thickness is determined by vernier caliper. Gold wires (50 µm) were attached on the upper and lower sides of the pellet with silver paste, and then the gold wires were fixed on the device with four electrodes. The impedance spectra obtained from the test were analyzed and fitted with Zview II (Scribner Associates). The total resistance (R) of the material was got by arc extrapolation to the Z′ axis from the Nyquist plots. The proton conductive (σ, $S\cdot m^{-1}$) was calculated by the common equal: $\sigma = L / (RS)$, where L, R, S mean the thickness of sample, total resistance and cross sectional area, respectively. Activation energy (Ea) values were determined from the Arrhenius equation between the conductive data 50 to 80 °C at 98% RH; 45 to 85 °C at 70% : $\ln (T\sigma) = \ln A - Ea / (k_B T)$, where T, k_B, A is absolutely temperature, boltzmann constant and pre-exponential factor, respectively.

Table S2. The proton conductivities ($S \cdot cm^{-1}$) of MOF under various RHs and 50°C.

RH	σ50°C/$S \cdot cm^{-1}$
60%	2.24×10^{-7}
65%	2.71×10^{-7}
70%	3.56×10^{-7}
75%	5.50×10^{-7}
80%	1.12×10^{-6}
85%	2.84×10^{-6}
90%	7.94×10^{-6}
98%	7.92×10^{-5}

Table S3. The proton conductivities (S·cm^{-1}) of others MOFs under various RHs and temperature.

Compounds	Conducting medium	Condition	Conductivity/ S·cm^{-1} (Ea)	Type of design	Reference
Im-Cu@NENU-3a$[Cu_{12}(BTC)_8(H_2O)_{12}][HPW_{12}O_{40}]$	H_2O, coordinated imidazole	70 °C, 90% RH	3.16×10^{-4} (0.79 eV)	functional group	2
Im@NENU-3$[Cu_{12}(BTC)_8(H_2O)_{12}][HPW_{12}O_{40}]$	H_2O, Guest imidazole	70 °C, 90% RH	1.82×10^{-2} (0.34 eV)	imidazole guest inclusion	2
*bio*MOF $\{Ca^{II}Cu^{II}_6[(S,S)\text{-}alamox]_3(OH)_2(H_2O)\}\cdot 32H_2O$	H_2O	80 °C, 95% RH	8.6×10^{-4} (0.34 eV)	H_2O guest	3
Im−Fe−MOF	coordinated imidazole	25 °C, 98% RH	2.06×10^{-3} (0.44 eV)	functional group	4
Im@Fe−MOF	uncoordinated imidazole	25 °C, 98% RH	8.41×10^{-5} (0.44 eV)	imidazole guest inclusion	4
$\{(Tb(\mu_3\text{-}HPhIDC)(\mu_2\text{-}C_2O_4)_{0.5}(H_2O))\cdot 2H_2O\}_n$	H_2O; uncoordinated N	100 °C, 98% RH	8.95×10^{-4} (0.45 eV)	H_2O guest	5
$\{(Eu(\mu_3\text{-}HPhIDC)(\mu_2\text{-}C_2O_4)_{0.5}(H_2O))\cdot 2H_2O\}_n$	H_2O; uncoordinated N	100 °C, 98% RH	4.63×10^{-4} (0.28 eV)	H_2O guest	5
Im@$[Al(\mu_2\text{-}OH)(1,4\text{-}ndc)$	imidazole	120 °C	2.2×10^{-5} (0.6 eV)	imidazole guest inclusion	6
H_2O-HKUST-1	H_2O	25 °C	1.5×10^{-5}	guest inclusion	7
EtOH-HKUST-1 or MeCN-HKUST-1	EtOH or MeCN	25 °C	2×10^{-7}	guest inclusion	7
Pristine-HKUST-1	H_2O	25 °C	5.0×10^{-7}	functional group	7
UiO-66$(SH)_2$	-SH	80 °C, 90% RH	2.5×10^{-5} (0.23 eV)	functional group	8
UiO-66$(SO_3H)_2$	$-SO_3H$	80 °C, 90% RH	8.4×10^{-2} (0.32 eV)	functional group	8

im@UiO-67	imidazole	120 °C	1.44×10^{-3} (0.36 eV)	imidazole guest inclusion	9
[Zn$_2$(2,5-dihydroxyterephthalic acid)]$_n$ -His	histamine	146 °C	4.3×10^{-9} (0.36 eV)	histamine guest inclusion	10

Table S4. Summary of earlier reported MOF structures with sulphate and organic ligands.

Compound	Ligands/Linkers	M-SO_4 chains	Network dimension	Reference
$Cu_2(SO_4)_2(DHBDI)_3$	sulphate/imidazole	yes	3D	this work
$[Co_4(SO_4)_3(F)_3(tpt)_2(tatb)]$	sulphate/fluoride/carboxylate	no	3D	11
$[Mn(L)_2](SO_4)_{16}H_2O$ (**1**), $[Cd_3(L)_2(SO_4)_4(H_2O)_2(EtOH)_2][Cd(H_2O)_6]_2H_2O$ (**2**)	sulphate/imidazole	no	2D	12
VNU-15	sulphate/carboxylate	yes	3D	13
$[\{Cu_3(OH)\}_2(SO_4)_5(H_2O)_{2\{}tr_3ad\}_3]\cdot 26H_2O$	sulphate/triazole	no	2D	14
$[Zn_2(trz)(SO_4)(OH)]$(**1**), $[Cd_8(trz)_4(OH)_2(SO_4)_5(H_2O)]$ (**2**)	sulphate/triazolate	yes	3D	15
$[Cu_4(L)_4(SO_4)_4]\cdot 4[Cu(H_2O)_6(SO_4)]$ (**1**), $[Cu_6(L)_3(SO_4)_5(OH)_2(H_2O)_6]\cdot 13H_2O$(**2**)	sulphate/triazole	yes	3D	16
$\{[Cu_6(atr)_6(H_2O)_2(\mu_3\text{-}OH)_2(SO_4)_5]\cdot 5.25H_2O\}_n$ (**1**), $\{[Cu_2(atr)_2(\mu\text{-}OH)_2(SO_4)]\cdot 3H_2O\}_n$ (**2**) $\{[Cu_7(atr)_6(H_2O)_6(\mu_3\text{-}OH)_2(SO_4)_6]\cdot 2H_2O\}_n$ (**3**)	sulphate/triazolate	yes	2D	17
$Cu_4(OH)(SO_4)_3(4\text{-}PmBC)(DMF)]$ $0.5DMF\cdot 3H_2O$	sulphate/pyrimidine/carboxylate	no	3D	18
$[Zn_2(Htrb)_{0.5}(L1)(SO_4)]\cdot H_2O$ (**1**), $[Zn_{1.5}(Htrb)_{0.5}(L2)_{0.5}(SO_4)]\cdot 5H_2O$ (**2**), $[Zn_3(Htrb)(SO_4)_3(H_2O)_3]\cdot H_2O$ (**3**),	sulphate/triazolate	no	3D	19

Reference

1. P. Kumar and J. Sahoo, *Oriental Journal of Chemistry*, 2014, **30**, 211-217.
2. Y. Ye, W. Guo, L. Wang, Z. Li, Z. Song, J. Chen, Z. Zhang, S. Xiang and B. Chen, *J. Am. Chem. Soc.*, 2017, **139**, 15604-15607.
3. T. Grancha, J. Ferrando-Soria, J. Cano, P. Amorós, B. Seoane, J. Gascon, M. Bazaga-García, E. R. Losilla, A. Cabeza, D. Armentano and E. Pardo, *Chem. Mater.*, 2016, **28**, 4608-4615.
4. F. M. Zhang, L. Z. Dong, J. S. Qin, W. Guan, J. Liu, S. L. Li, M. Lu, Y. Q. Lan, Z. M. Su and H. C. Zhou, *J. Am. Chem. Soc.*, 2017, **139**, 6183-6189.
5. R. L. Liu, W. T. Qu, B. H. Dou, Z. F. Li and G. Li, *Chem Asian J*, 2020, **15**, 182-190.
6. S. Bureekaew, S. Horike, M. Higuchi, M. Mizuno, T. Kawamura, D. Tanaka, N. Yanai and S. Kitagawa, *Nat Mater*, 2009, **8**, 831-836.
7. N. C. Jeong, B. Samanta, C. Y. Lee, O. K. Farha and J. T. Hupp, *J. Am. Chem. Soc.*, 2012, **134**, 51-54.
8. W. J. Phang, H. Jo, W. R. Lee, J. H. Song, K. Yoo, B. Kim and C. S. Hong, *Angew. Chem. Int. Ed. Engl.*, 2015, **54**, 5142-5146.
9. S. Liu, Z. Yue and Y. Liu, *Dalton Trans*, 2015, **44**, 12976-12980.
10. M. Inukai, S. Horike, D. Umeyama, Y. Hijikata and S. Kitagawa, *Dalton Trans*, 2012, **41**, 13261-13263.
11. T. Liu, X. Shen, X. Shen, C. He, J. Liu and J.-J. Liu, *CrystEngComm*, 2021, **23**, 4667-4673.
12. J. Fan, B. Sui, T.-a. Okamura, W.-Y. Sun, W.-X. Tang and N. Ueyama, *J. Chem. Soc., Dalton Trans.*, 2002, DOI: 10.1039/b202138b, 3868-3873.
13. T. N. Tu, N. Q. Phan, T. T. Vu, H. L. Nguyen, K. E. Cordova and H. Furukawa, *J. Mater. Chem. A*, 2016, **4**, 3638-3641.
14. G. A. Senchyk, A. B. Lysenko, I. Boldog, E. B. Rusanov, A. N. Chernega, H. Krautscheid and K. V. Domasevitch, *Dalton Trans*, 2012, **41**, 8675-8689.
15. W. Ouellette, B. S. Hudson and J. Zubieta, *Inorg. Chem.*, 2007, **46**, 4887-4904.
16. A. Dauth and J. A. Love, *Dalton Trans*, 2012, **41**, 7782-7791.
17. E. Yang, X. Wang, C. Zhang, N. Yang, Z. Liu and X. Zhao, *Science China Chemistry*, 2013, **56**, 465-474.
18. J. Luo, J. Wang, G. Li, Q. Huo and Y. Liu, *Chem Commun (Camb)*, 2013, **49**, 11433-11435.
19. Z. Zhang, J.-F. Ma, Y.-Y. Liu, W.-Q. Kan and J. Yang, *CrystEngComm*, 2013, **15**.